Optical signal degradation study in fixed human skin using confocal microscopy and higher-harmonic optical microscopy

Tsung-Han Tsai and Shih-Peng Tai

Department of Electrical Engineering and Graduate Institute of Electro-Optical Engineering, National Taiwan University, Taipei 10617, Taiwan

Wen-Jeng Lee

Department of Electrical Engineering, National Taiwan University and Department of Medical Imaging, National Taiwan University Hospital, Taipei 10051, Taiwan

Hsin-Yi Huang

Department of Dermatology, National Taiwan University Hospital, Taipei 10051, Taiwan

Yi-Hua Liao

Department of Pathology, National Taiwan University Hospital, Taipei 10051, Taiwan

Chi-Kuang Sun*

Department of Electrical Engineering and Graduate Institute of Electro-Optical Engineering, National Taiwan University, Taipei 10617, Taiwan

sun@cc.ee.ntu.edu.tw

Abstract: Confocal and nonlinear optical microscopies have been applied for dermatological studies because of their capability to provide sub-surface three-dimensional images with sub-μm spatial resolutions. Optical signal degradation as the imaging plane being moved toward deeper regions in skin specimens is the key factor that limits the observation depth for the laser scanning based linear or nonlinear imaging modalities. In this article, we studied the signal degradation in fixed human skin specimens using reflection confocal microscopy and higher-harmonic optical microscopy based on a Cr:forsterite femtosecond laser centered at 1230-nm. By analyzing the optical properties through these linear and nonlinear imaging modalities, we found that the optical signal degradation in the studied human skin specimen is dominated by the distortion of the point spread function.

OCIS codes: (170.1870) Dermatology; (180.6900) Three-dimensional microscopy; (180.5810) Scanning microscopy; (170.1790) Confocal microscopy; (190.4160) Multiharmonic generation

References and Links

1. G. J. Tearney, M. E. Brezinski, B. E. Bouma, S. A. Boppart, C. Pitris, J. F. Southern, and J. G. Fujimoto, "In vivo endoscopic optical biopsy with optical coherent coherent tomography," Science **276**, 2037-2039 (1997).
2. Y. Yasuno, S. Makita, Y. Sutoh, M. Itoh, and T. Yatagai, "Birefringence imaging of human skin by polarization-sensitive spectral interferometric optical coherent tomography," Opt. Lett. **27**, 1803-1805 (2002).
3. B. Povazay, K. Bizheva, A. Unterhuber, B. Hermann, H. Sattmann, A. F. Fercher, W. Drexler, A. Apolonski, W. J. Wadsworth, J. C. Knight, P. St. J. Russell, M. Vetterlein, and E. Scherzer, "Submicron axial resolution optical coherence tomography," Opt. Lett. **27**, 1800-1802 (2002).
4. M. Minsky, Microscopy apparatus. U.S. Patent 03013467 (1957).

#9917 - $15.00 USD Received 9 December 2005; revised 17 January 2006; accepted 18 January 2006

5. C. J. R. Sheppard and D. M. Shotton, Confocal Laser Scanning Microscopy (BIOS Scientific Publisher, Oxford, 1997).
6. P. T. C. So, H. Kim, and I. E. Kochevar, "Two photon deep tissue ex vivo imaging of mouse dermal and subcutaneous structures," Opt. Express **3**, 339-350 (1998).
7. B. R. Masters and P. T. C. So, "Confocal microscopy and multi-photon excitation microscopy of human skin in vivo," Opt. Express **8**, 2-10 (2001).
8. Y. Guo, P. P. Ho, H. Savage, D. Harris, P. Sacks, and S. Schantz, F. Liu, N. Zhadin, and R. R. Alfano, "Second-harmonic tomography of tissues," Opt. Lett. **22**, 1323-1325 (1997).
9. C.-K. Sun, C.-C. Chen, S.-W. Chu, T.-H. Tsai, Y.-C. Chen, and B.-L. Lin, "Multi-harmonic generation biopsy of skin," Opt. Lett. **28**, 2488-2490 (2003).
10. S.-P. Tai, T.-H. Tsai, W.-J. Lee, D.-B. Shieh, Y.-H. Liao, H.-Y. Huang, K. Y.-J. Zhang, H.-L. Liu, and C.-K. Sun, "Optical biopsy of fixed human skin with backward-collected optical harmonics signals," Opt. Express **13**, 8231-8242 (2005).
11. B. Selkin, M. Rajadhyaksha, S. González, and R. G. Langley RG, "In vivo confocal microscopy in dermatology," Dermatol. Clin. **19369–77**, ix-x (2001).
12. M. Rajadhyaksha, M. Grossman, D. Esterowitz, R. H. Webb, R. R. Anderson, "In vivo confocal scanning laser microscopy of human skin: melanin provides strong contrast," J. Invest. Dermatol. **104**, 946-952 (1995).
13. J. A. Veiro, and P. G. Cummins, "Imaging of skin epidermis from various origins using confocal laser scanning microscopy," Dermatology **189**: 16-22 (1994).
14. W. Denk, J. H. Strickler, W. W. Webb, "Two-photon laser scanning fluorescence microscopy," Science **248**, 73-76 (1990).
15. V. R. Daria, C. Saloma, and S. Kawata, "Excitation with a focused, pulsed optical beam in scattering media: diffraction effects," Appl. Opt. **39**, 5244-5255 (2000).
16. M. Gu, X. Gan, A. Kisteman, and M. G. Xu, "Comparison of penetration depth between two-photon excitation and single-photon excitation in imaging through turbid tissue media," Appl. Phys. Lett. **77**, 1551-1553 (2000).
17. A. Egner and S. Hell, "Equivalence of the Huygens-Fresnel and Debye approach for the calculation of high aperture pointspread functions in the presence of refractive index mismatch," J. Microsc. **193**, 244-249 (1999).
18. R. R. Anderson, and J. A. Parrish, "The optics of human skin," J. Invest. Dermatol. **77**, 13-19 (1981).
19. C.-K. Sun, S.-W. Chu, S.-Y. Chen, T.-H. Tsai, T.-M. Liu, C.-Y. Lin, and H.-J. Tsai, "Higher harmonic generation microscopy for developmental biology," J. Struct. Bio. **147**, 19-30 (2004).
20. S.-W. Chu, S.-Y. Chen, T.-H. Tsai, T.-M. Liu, C.-Y. Lin, H.-J. Tsai, and C.-K. Sun, "In vivo developmental biology study using noninvasive multi-harmonic generation microscopy," Opt. Express **11**, 3093-3099 (2003).
21. P. N. Prasad, Introduction to Biophotonics (John Wiley & Sons, Hoboken, 2003).
22. S.-W. Chu, I-H. Chen, T.-M. Liu, P. C. Cheng, C.-K. Sun, and B.-L. Lin, "Multimodal nonlinear spectral microscopy based on a femtosecond Cr:forsterite laser," Opt. Lett. **26**, 1909-1921 (2001).
23. D. Yelin and Y. Silberberg, "Laser scanning third-harmonic-generation microscopy in biology," Opt. Express **5**, 169-175 (1999).
24. J. A. Squier, M. Muller, G. J. Brakenhoff, and K. R. Wilson, "Third harmonic generation microscopy," Opt. Express **3**, 315-324 (1999).
25. P. J. Campagnola, A. C Millard, M. Terasaki, P. E. Hoppe, C. J. Malone, and W. A. Mohler, "Three-dimensional high-resolution second-harmonic generation imaging of endogenous structural proteins in biological tissues," Biophy. J. **81**, 493-508 (2002).
26. S.-W. Chu, I-S. Chen, T.-M. Liu, C.-K. Sun, S.-P. Lee, B.-L. Lin, P.-C. Cheng, M.-X. Kuo, D.-J. Lin, and H.-L. Liu, "Nonlinear Bio-photonic Crystal Effects Revealed with Multi-modal Nonlinear Microscopy," J. Microsc. **208**, **Part 3**, 190-200 (2002).
27. H. Elias, J. E. Pauly, and E. R. Burns, Histology and Human Microanatomy, 4th Edition, Piccin Medical Books (Wiley, New York, 1978).
28. M. Rajadhyaksha, S. González, J. M. Zavislan, R. R. Anderson, and R. H. Webb, "In vivo confocal scanning laser microscopy of human skin II: Advances in instrumentation and comparison with histology," J. Invest. Dermatol. **113**, 293-303 (1999).
29. S. González and Z. Tannous, "Real-time, in vivo confocal reflectance microscopy of basal cell carcinoma," J. Am. Acad. Dermatol. **47**, 869-874 (2002).
30. T. Yamashita, T. Kuwahara, S. González, and M. Takahashi, "Non-invasive visualization of melanin and melanocytes by reflectance-mode confocal microscopy," J. Invest. Dermotal. **124**, 235-240 (2005).
31. A. Dunn and R. Richards-Kortum, "Three-dimensional computation of light scattering from cells," IEEE J. Sel. Top. Quantum Electron. **2**, 898-905 (1996).
32. H. Beyer, Handbuch der Mikroskopie, 2nd Edition (VEB Verlag Technik, Berlin, 1985).

#9917 - $15.00 USD Received 9 December 2005; revised 17 January 2006; accepted 18 January 2006

33. J. Squier, and M. Müller, "High resolution nonlinear microscopy: A review of sources and methods for achieving optimal imaging," Rev. Sci. Instrum. **72**, 2855-2867 (2001).
34. J. Mertz and L. Moreaux, "Second-harmonic generation by focused excitation of inhomogeneously distributed scatterers," Opt. Comm. **196**, 325-330 (2001).
35. W.H. Press, S.A. Teukolsky, W.T. Vetterling, and B.P. Flannery, Numerical Recipes in C (Cambridge Univ. Press, Cambridge, 1992).

1. Introduction

Optical imaging and microscopy such as optical coherence tomography (OCT) [1-3], confocal microscopy [4,5], and nonlinear optical microscopy [6-10] have been widely applied for dermatological studies because of their high penetration and three-dimensional (3D) imaging capability with high spatial resolutions. OCT can provide high penetration using 1.3-μm wavelength light [1] or a sub-μm axial resolution with a 725-nm broadband light source [3]. Compared with OCT, laser scanning confocal and nonlinear microscopies provide much higher lateral resolution while the sectioned two-dimensional images are in the plane parallel to the surface, in contrast to the cross-sectional (tangential) images provided by OCT. Reflection confocal microscopy has provided a window into living skin for basic and clinical research. Confocal reflectance images of normal skin correlate well with images from conventional histology, with contrast being provided by refractive index differences of subcellular structures such as cell layers and nuclear details in the epidermis, collagen, and microcirculation in the dermis [11-13]. It was also found that pigmented skin and pigmented lesions are especially suitable for laser scanning confocal microscopy because melanin functions as a natural source of contrast [12]. Two-photon fluorescence microscopy [14] of skin based on 780-nm femtosecond light also provides high resolution imaging from the skin surface through the epidermal-dermal junction [7]. Recently we demonstrated that higher-harmonic optical microscopy (HOM) based on a 1230-nm femtosecond light source could provide sub-micrometer-resolution deep-tissue biopsy images of skin without the use of fluorescence or exogenous markers [9,10], which could also be considered as a powerful tool for dermatological studies.

Optical signal degradation as the imaging plane being moved toward deeper regions in skin specimens is the key factor that limits the observation depth for the laser scanning based linear or nonlinear imaging modality mentioned above. The signal degradation in biological tissues might probably be owing to the excitation light attenuation, the distortion and broadening of the 3D excitation point spread function (PSF), and the broadening of the femtosecond excitation light pulses [15,16]. The refractive index differences in tissues, which are significant for lenses with high numerical apertures (NA), cause not only aberration effects that distort the PSF profiles [17], but are also responsible to move part of the incident light away from the focal spot, which can be considered as part of the scattering loss. Due to the combination of scattering and absorption, the average power delivered at the focal plane also attenuates with increasing depth, as predicted by the Beer's law. While the broadening of the femtosecond pulsewidth will severely reduce the generated nonlinear signals, the reduced average excitation power and the distorted PSF would reduce both the linear and nonlinear optical signal intensities, smooth the image details with poorer imaging resolutions, and degrade the relative contrast of the generated images.

In this article, we studied the signal degradation of linear and nonlinear imaging modalities in fixed human skin specimens using reflection confocal microscopy and HOM based on a Cr:forsterite femtosecond laser centered at 1230-nm. By minimizing the combined effects of scattering and absorption of common tissue constituents such as water, melanin, and hemoglobin, 1.3-μm light is known to provide the deepest penetration capability in live

#9917 - $15.00 USD Received 9 December 2005; revised 17 January 2006; accepted 18 January 2006

biological specimens [1,18-20]. By analyzing the optical properties through reflection confocal (RC), second harmonic generation (SHG), and third harmonic generation (THG) modalities including spatial resolutions and measured signal power at different imaging depths in fixed human skin specimens, we show that the optical signal degradation in the studied human skin specimens with a light source in the optical penetration window is dominated by the distortion induced broadening of the point spread function, rather than light attenuation or femtosecond pulse-broadening.

2. Materials and methods

The study of the signal degradation in fixed human skin specimen was performed with a femtosecond Cr:forsterite laser centered at 1230-nm with a 140-fs pulse width at a 110-MHz repetition rate, using a harmonic laser scanning microscope combining RC microscopy (that could be considered as the fundamental harmonic mode) with higher-harmonic modalities, as shown in Fig. 1. The 1230 nm infrared (IR) laser beam was first shaped by a telescope and then directed into a modified beam scanning system (Olympus Fluoview 300) and a microscope (Olympus BX-51) with an IR water-immersion objective (LUMplanFL/IR 60X/NA 0.9). The RC signals were collected in the reflection geometry by use of the same objective. The reflection 1230 nm signal passed through the same scanner and a confocal pinhole with the size of 0.25-AU (1-AU=1.22λ/NA) [21] and was detected by an IR-sensitive photodetector (PDA400, Thorlabs). With a momentum conservation law, most of the SHG and THG photons are with a forward propagating characteristic. We collected the forward transmitted SHG (615 nm light) and THG (410 nm light) signals by a 1.4-NA achromatic visible condenser, divided them by a chromatic beam splitter, and detected them by two separate photomultiplier tubes with 410- and 615-nm narrowband interference filters in front. Average illumination power of 90-mW was applied to the sample surface during the study.

The fixed integument samples were removed from the back of a seventy-year-old female patient and preserved in formalin at 4□. The experimental protocols were approved the National Taiwan University Hospital Institutional Review Board (NTUH-IRB). The thickness of the samples under observation was on the order of 1 mm.

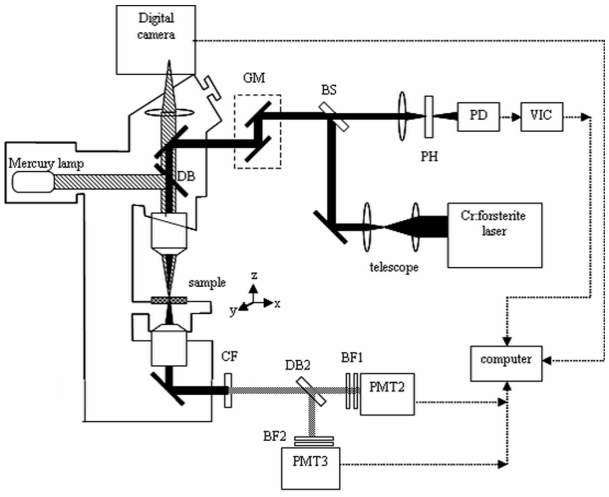

Fig. 1. Set up of the harmonic laser scanning microscope combining the reflection confocal with the higher-harmonic generation modalities. BF: barrier filter; BS: beamspliter; DB: dichroic beamsplitter; PMT: photomultiplier tube; GM: galvanometric mirrors; PD: photodetector; VIC: V-I converter circuit; PH: confocal pinhole.

#9917 - $15.00 USD Received 9 December 2005; revised 17 January 2006; accepted 18 January 2006

3. Experimental results and discussion

Figure 2 and Fig. 3 show examples of the cross-sectional images taken at depths of 90- and 150-μm from the studied skin surface by the harmonic laser scanning microscope. With the signals oriented from refractive index differences, RC can reflect subcellular structures such as cell layers and nuclear details in the epidermis, as well as collagens and microcirculation in the dermis [12,13] while the general histological structures in both epidermis and dermal layers can also be identified through the THG modality due to its sensitivity to local optical inhomogeneities [22-24], including refractive index (or susceptibility $\chi^{(1)}$) and third-order susceptibility $\chi^{(3)}$ differences which usually occurs at the same bio-locations. Fig. 2(a) and Fig. 2(B) show cross-sectional RC and THG images in the stratum basal layer on top of the dermo-epidermal junction. The highly-correlated images of the densely packed basal cells resolved by the RC and THG signals clearly indicate that the RC and THG modalities have the similar sources of contrast in human skin, i.e., optical susceptibility discontinuities. In the dermal layer, as shown Fig. 3(a), RC signals can still pick up fine structures including wavy collagen fibril distribution in the connective tissues with relatively less brightness than the RC image shown in Fig. 2(a). THG signals, on the other hand, decreases more significantly deep into the dermal layer (see Fig. 3(b)), compared with the linear-optics based RC signals [16]. With strong optical second harmonic generation in collagen fibers [8,25,26], the SHG modality provides the unique capability to reflect the distribution of connected tissues in the dermal layer [10] (Fig. 3(c)). The uneven distribution of SHG signals in Fig. 2(c) is due to the *Rete ridge* structures of the dermal papillae [27] inter-digitated with the downward projections of the epidermis.

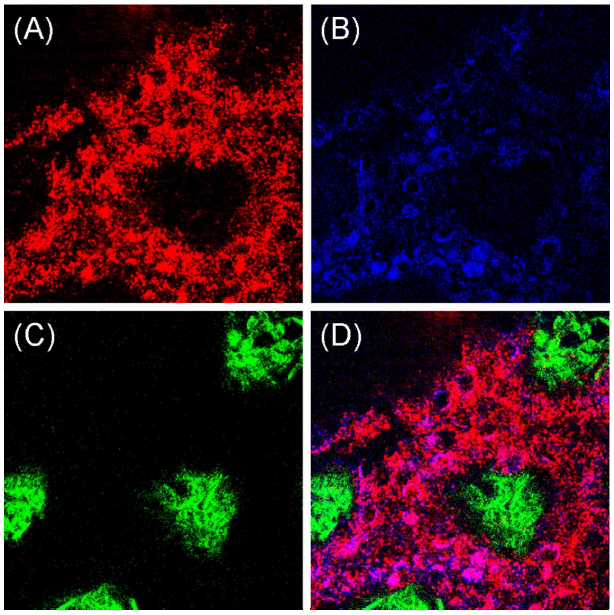

Fig. 2. Cross-sectional (a) RC, (b) THG, (c) SHG, and (d) combined images of human skin taken at a depth of 90-μm from the skin surface around the dermo-epidermal junction. Images size: 120x120μm.

#9917 - $15.00 USD Received 9 December 2005; revised 17 January 2006; accepted 18 January 2006

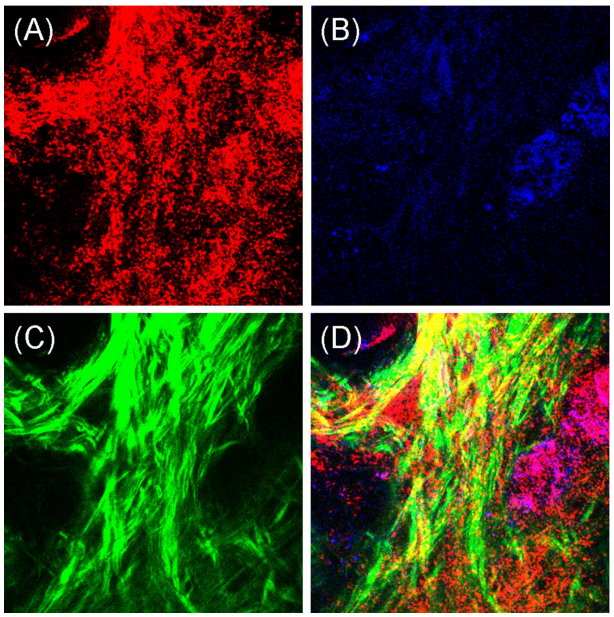

Fig. 3. Cross-sectional (a) RC, (b) THG, (c) SHG, and (d) combined images of human skin taken at a depth of 150-μm from the skin surface in the dermal layer. Images size: 120x120μm.

Previous studies in the epidermis layers of human skins with the RC microscopy have already proved that the bright areas in confocal images (Fig. 2(a)) are cytoplasm and the dark areas within are the nuclei of the viable epidermis [11]. Previous RC images in human skin [11-13, 28-30] provided very helpful evidences that the light scatterings from basal cells is dominated by the scattering of organelles inside [31]. With a high correlation between the RC and THG signals in the basal cells (Fig. 2 (d)), our comparison study suggests that the THG signals in the basal layers of human skin reflect the locations of the cytoplasm that containing melanin and multiple organelles, similar to that of the RC signals [12]. Therefore, the round-shaped dark THG images in basal cells (Fig. 2(b)) allow the observation of nuclei in basal cells with higher spatial resolution compared with the RC imaging modality, while distinguishing the shapes, distributions, and sizes of the nuclei in basal cells is essential for the diagnosis of skin cancer.

The lateral resolution degradation of different imaging modalities can be estimated by analyzing the fine structures of the obtained images. Figure 4 shows the obtained lateral resolution of these three imaging modalities at different imaging depths inside the studied human skin specimen. Note that there are no collagen fibrils in the epidermis at the depth shallower than 75-μm relative to the surface of the skin sample, so the lateral resolution of SHG modality at the 75-μm depth is not shown. On the other hand, the THG signal is too weak to detect at a depth of more than 300-μm relative to the surface of the skin, hence the lateral resolution of the THG modality at a 300-μm depth is not shown either. The focal diameters of the incident laser beam versus depth can then be derived according to the observed resolution of the RC, the SHG, and the THG images as shown in Fig. 5 with the related resolution formula [21,32,33] listed in Table 1. The well-matched focal diameters derived from these different imaging modalities support the accuracy of the derived data. The derived focal diameter close to the sample surface matches well the theoretical value based on optical diffraction. It is important to notice that the results shown in this study are independent of the sample thickness. By increasing the sample thickness, the obtained SHG or THG images at different focusing depths will all experience the same signal attenuation due to the

#9917 - $15.00 USD Received 9 December 2005; revised 17 January 2006; accepted 18 January 2006

constant SHG or THG attenuation in the extra sample layer. The image resolution study shown in Fig. 4 and Fig. 5 is independent of the signal intensity, and is thus independent of the sample thickness. For the signal degradation study which will be presented next, the constant SHG or THG signal attenuation due to the extra sample layer will be cancelled since the analysis results are only dependent on the relative signal powers at different imaging depths.

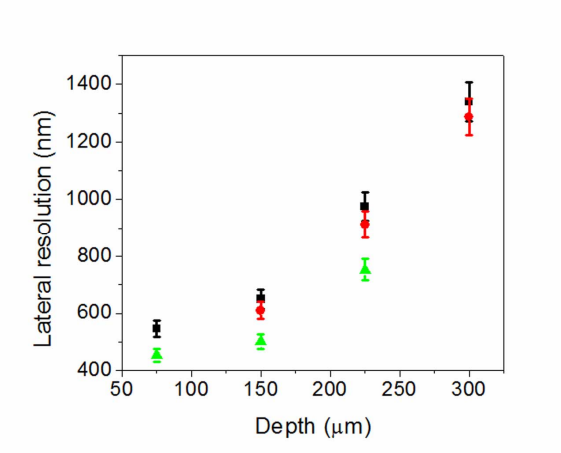

Fig. 4. Lateral resolutions of RC (black square), SHG (red circle), and THG (green triangle) images versus depth in the studied human skin sample.

Table 1. Formula for the focal beam diameter and the resolutions of different imaging modalities.

Beam diameter	**RC resolution**	**SHG resolution**	**THG resolution**
$\frac{0.51\lambda}{NA}$	$\frac{0.37\lambda}{NA}$	$\frac{0.36\lambda}{NA}$	$\frac{0.3\lambda}{NA}$

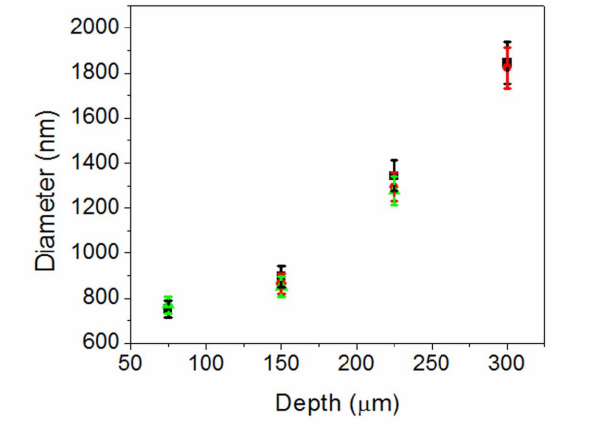

Fig. 5. Focal diameter degradation with depth in the studied human skin sample derived from the lateral resolution of the RC (black square), SHG (red circle), and THG (green triangle) images respectively.

#9917 - $15.00 USD Received 9 December 2005; revised 17 January 2006; accepted 18 January 2006

The incident light peak intensity at the focal plane is the critical factor to the generation of signals, especially to nonlinear SHG and THG signals. Because of nonlinearity, the generated SHG intensity depends on the square power of the incident light intensity, while the generated THG intensity depends on the third power of the incident light intensity. When the incident light peak intensity decreases, the generated SHG and THG intensities will also severely decay. Due to distortion of the point spread functions as the observation depth move to deeper regions, the focal area also get larger that causes the reduction of the proportional RC signals that passing through the confocal pinhole. Therefore, the measured RC signal power would be inversely proportional to the focal area, that is, inversely quadratic to the focal diameter [32]. Since the generated THG intensity depends on the third power of the incident light intensity and the measured signal intensity depends on inversely quadratic of the focal diameter of the incident light, the THG signal intensity depends on the inverse 6^{th} power of the focal diameter of the incident light. The THG signal power thus depends on inversely quartic (inverse 4^{th} power) of the focal diameter of the incident light. Figure 6 shows the collected RC signal power versus focal diameter taken at different sample depths. The values of the focal diameters at different sample depths are based those shown in Fig. 5. We did not analyze the power dependency of the SHG signal because the intensity of the forward SHG signal is strongly dependent on the collagen fibril thickness [10,34] while the thickness of the collagen fibrils in the dermis layer is very uneven. The distribution of the SHG signal is also very different from those of RC and THG signals. Collagen-induced SHG is only present in the dermal layer [10] and its uneven signal distribution is further modified by the *Rete ridge* structures of the dermal papillae [27] inter-digitated with the downward projections of the epidermis. Based on a chi-square-based fitting method [35] (solid black line in Fig. 6), the dependency of the RC signal power on the focal diameter broadening as the focal plane moving into the sample can be found to be roughly negatively quadratic with a slope of -2.24, confirming that the degradation of signal power is mainly affected by the distortion of the focused beam size in our study. The difference between slope = -2.24 and slope = -2 in Fig. 6 could be attributed to the attenuation of optical signals in the skin specimen, which is another important signal degradation mechanism. Pulse broadening will not affect the intensity of the RC signals. Based on this assumption, we could also obtain an effective attenuation coefficient of 6.3-cm^{-1} (for 1230-nm light) based on analyzing the difference of these two slopes. The effective attenuation coefficient α for 1230-nm light was calculated according to the Beer's law, i.e., $\alpha = (\ln P_1 - \ln P_2)/2\Delta d$, where P_1 is the power calculated from the solid line with slope = -2 at the depth of Δd, P_2 is the power measured from the skin specimen at the depth of Δd, and the factor of 2 is due to the roundtrip measurement in the reflection geometry.

#9917 - $15.00 USD Received 9 December 2005; revised 17 January 2006; accepted 18 January 2006

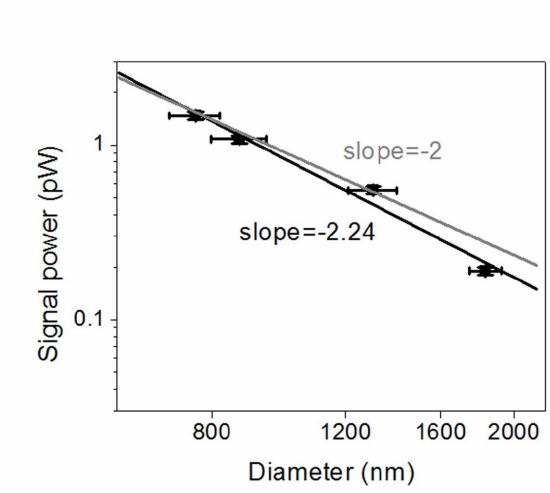

Fig. 6. RC signal power (square) versus focal diameter degradation with different depths in the studied human skin sample. The black solid line is the best fit with a slope = -2.24 and the gray solid line is the slope = -2 fitting. Note that both axes are log-scaled.

Figure 7 shows the dependency of the THG signal power on the focal diameter degradation as the focal plane moving into the sample, where the solid black line is the best fit obtained based on a chi-square-based fitting method [34] with a slope of -4.5, confirming that the degradation of THG signal power is also mainly affected by the distortion of the focused beam size. Compared with the ideal case with a slope of -4 where only the distortion of the point spread function is considered, the slight difference between the experimental data and the theoretical upper limit (-4.5 versus -4) could be attributed to light attenuation and the broadening of the femtosecond pulsewidth. When the imaging depth was increased with Δd, the average intensity of the 1230nm excitation light would be decreased with a factor of $e^{\alpha\Delta d}$, while the generated THG average intensity at the focal spot would be decreased with a factor of $e^{3\alpha\Delta d}$, assuming that the excitation pulsewidth was not broadened. With a forward collection geometry and an increasing excitation depth, the total propagation length for THG photons will be decreased. With a THG photon attenuation constant α', the measured THG intensity should thus experience a degradation factor of $e^{(3\alpha-\alpha')\Delta d}$, due to the light attenuation effect. Due to stronger light attenuation at 410 nm than that at 1230 nm [18], the signal degradation due to the light attenuation effect in forward THG study should thus be weaker than the RC study (with a factor of $e^{2\alpha\Delta d}$). The relatively stronger discrepancy in the THG study (-4.5 versus -4), compared with the result in the RC study (-2.24 versus -2), indicates the contribution of the femtosecond pulsewidth broadening to the observed nonlinear signal degradation. However our analysis suggests that the degradation of optical signal power versus imaging depth, for linear confocal or nonlinear imaging modalities in the studied human skin sample with a 1230-nm light in the optical penetration window, is dominated by the distortion induced focal diameter broadening rather than the light attenuation [16] or dispersion induced pulse broadening. This is understandable due to the fact that the applied laser wavelength is located in the optical penetration window of the studied specimens [18] and is close to the dispersion zero wavelengths of normal materials. Due to higher dependency of the nonlinear signal degradation on the focal diameter broadening, the nonlinear optical signal (for example THG) power will decay more rapidly while the observation plane moves deeper into the skin specimens.

#9917 - $15.00 USD Received 9 December 2005; revised 17 January 2006; accepted 18 January 2006

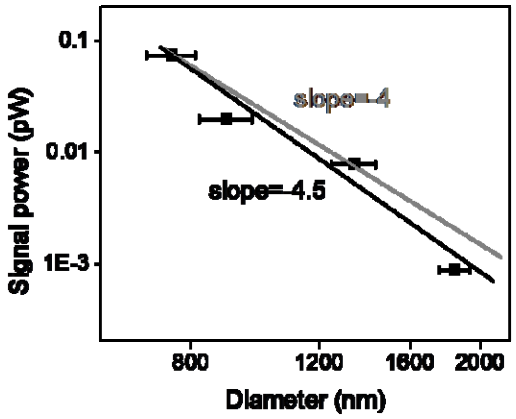

Fig. 7. THG signal power (square) versus focal diameter degradation with different depths in the studied human skin sample. The solid black line is the best fit with a slope = -4.5. The solid gray line is with a slope = -4. Note that both axes are log-scaled.

4. Conclusion

In summary, we studied the optical signal degradation mechanisms in fixed human skin specimens using RC microscopy and higher-harmonic optical microscopy based on a Cr:forsterite femtosecond laser centered at 1230-nm. By analyzing the optical properties through these linear and nonlinear imaging modalities, we found that the optical signal degradation in the studied fixed human skin specimen is primarily dominated by the distortion of the point spread function, while the excitation light attenuation or dispersion induced optical pulse broadening can be considered as secondary effects. The capability of THG modality to resolve the shapes, distribution, and sizes of nuclei in human skin basal cells with high spatial resolution could also provide an imaging solution for the diagnosis of skin cancer with minimized invasion.

Acknowledgments

The authors gratefully acknowledge financial support under the National Health Research Institute (NHRI-EX94-9201EI) of Taiwan and the National Taiwan University Center for Genomic Medicine.

#9917 - $15.00 USD Received 9 December 2005; revised 17 January 2006; accepted 18 January 2006